

FAR-OUT SIDELOBES IN LARGE REFLECTOR ANTENNAS

James Lamb

INTRODUCTION

Power scattered from the main beam into sidelobes can cause source confusion, increase the system noise and make the antenna sensitive to interference. Reasonable estimates of sidelobe levels and distribution need to be made so that the antenna design may be appropriately optimized. At worst about half of the power may be in the sidelobes while for an efficient antenna it may be around 10% or less. Typically, then, the average sidelobe level relative to isotropic is in the range -3 to -10dBi. There may be a much greater variation in the peak levels, however.

A major reason for power being scattered out of the main beam is obstructions in the aperture of the antenna. In a symmetrical antenna these blockages are generally inevitable and it is difficult to make any significant reduction in the scattering. Other scattering mechanisms, such as edge diffraction at the primary and secondary mirrors, may be reduced by using a narrower feed pattern, and the blockage will be the ultimate limiting factor. An off-set antenna avoids the blockage problem and the primary feed pattern will become a limiting factor. Both types of antenna are affected by gaps between panels, and by inaccuracies in the surface.

Although the off-set antenna is attractive from an electromagnetic standpoint it is perhaps less desirable mechanically. A quantitative comparison of the achievable sidelobes of the two is therefore necessary in order to see if the extra effort of the off-set design is justified. This note discusses various mechanisms for producing sidelobes and some attempts are made to assess quantitatively the limits on both types of antenna. Where the total scattered power is calculated it is given in terms of the fraction of the total power flowing through the aperture. Power densities are given relative to an isotropic radiator (which is equivalent to the standard directivity definition). Discussion of near-in sidelobes is limited to giving an estimate of the angular extent for the purposes of comparison, and the primary purpose is to investigate far-out sidelobes.

Antenna Models

Two antenna models will be used for sample calculations: the symmetric antenna of Fig. 1, and the off-set design of Fig. 2. A wavelength of 21cm is used

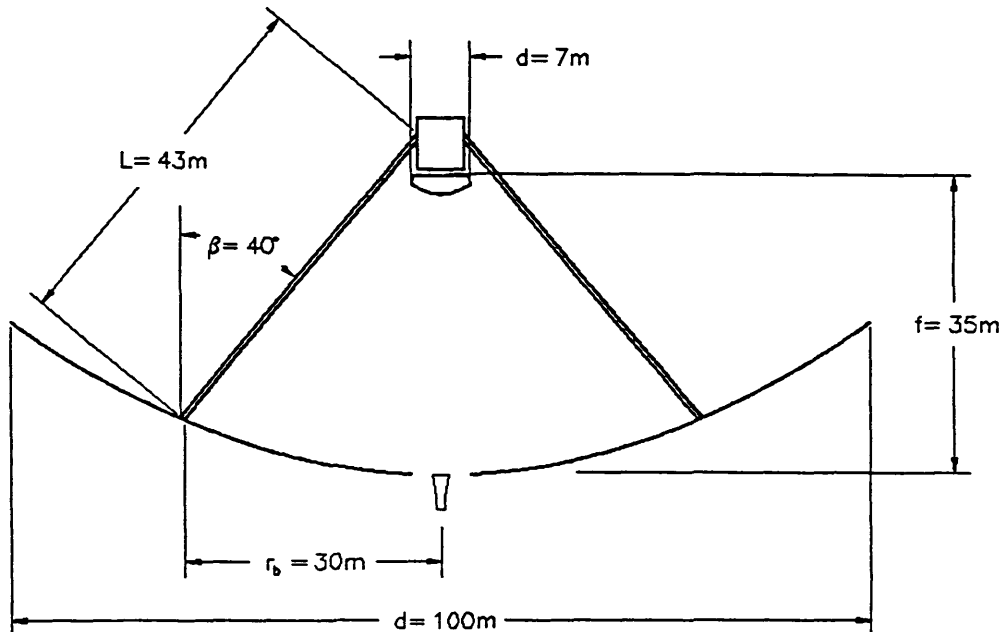


Figure 1 Parameters for axisymmetric antenna used in calculations in the text.

but most of the results may easily be recomputed for other values. Most of the calculations are very similar for the two antennas in the degree of approximation used here. The main differences are in the values of the focal ratios and the absence of strut blockage in the off-set design. (Note that the off-set is not completely free from blockage since there is some blockage of feed spillover round the primary.) For the purposes of this study it makes sense to define the focal ratio of the off-set as the distance from the focal point to the center of the reflector. The focal ratio is then roughly equal to the subtended angle at the feed.

NEAR IN SIDELOBES

Near-in sidelobes are defined by features in the aperture field which have a dimension of a few percent or more of the aperture diameter. This includes such things as the taper of the illumination over the aperture, and blockage by the secondary reflector and its support structure. An aperture which is uniformly

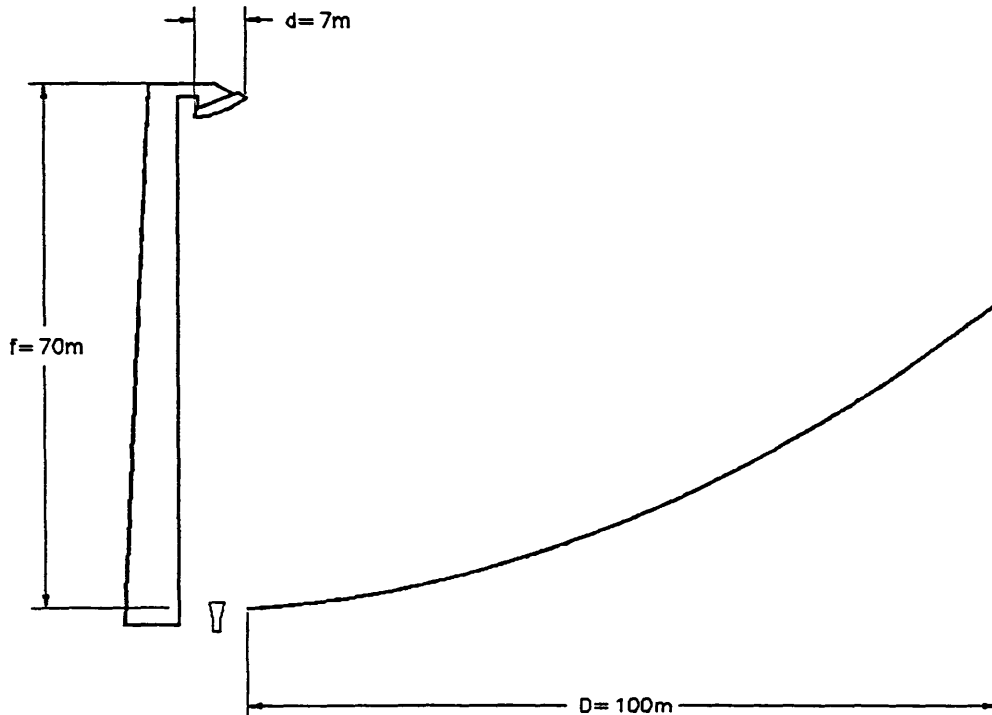


Figure 2 Parameter values for model off-set antenna.

illuminated and has no blockage will have sidelobes due to the sharp change in field at the edge of the aperture and the first lobe will have an amplitude of -17.6dB relative to the main beam. Tapering the amplitude towards the edge of the aperture will reduce this level, and generally it is below -20dB for single dish telescopes.

Blockage will introduce further sidelobes. Consider a circular central blockage of diameter d . Its effect may be found by looking at the diffraction pattern of a circular aperture of the same size. This pattern will be broader than the main beam by a factor of $\sim D/d$ where D is the diameter of the aperture, and its peak amplitude will be lower by a factor of $\sim (d/D)^2$. The radiation pattern of the telescope with the blockage is found by subtracting this field from the field of the unblocked aperture. Secondary reflectors normally have diameters of between $D/10$ and $D/20$ so the sidelobes due to the central blockage will be 10 to 20 times wider than the main beam, and the level relative to the on-axis beam will be -40 to -60dB . The central blocking will place a limit on how low the sidelobe levels can be made by narrowing the illumination pattern since the component due to the blockage will increase with increasing taper. Levels cannot be expected to be much below -40dB .

In the case of an unobscured aperture, such as found in the offset design, no extra sidelobes are produced by narrowing the illumination pattern but the main beam becomes much broader and resolution is reduced.

Near-in sidelobes are also produced by cross-polarization. These usually have a peak near the -10dB level of the main co-polar lobe.

Astigmatism, coma, and spherical aberration cause increases in the sidelobes very close to the main beam. Surface errors on a smaller scale with an rms of σ and a correlation distance of c will produce an error pattern with a width of [1]

$$\theta = 2 \sigma / c . \quad (1)$$

For a large precision antenna the error pattern will be within a few degrees of the main beam and therefore not contribute to the far-out sidelobes.

FAR-OUT SIDELOBES

Fig. 3 shows some of the mechanisms responsible for producing sidelobes in a typical telescope.

Feed Spillover

Sidelobes due to feed spillover will have the same distribution as the feed pattern at angles greater than that subtended by the reflector. The total power in the spillover pattern will be on the order of 10%, but the distribution will be dependent on the focal ratio. For a focal ratio of F/D , the sidelobe maximum falls at an angle of

$$\theta = 2 \tan^{-1} \frac{1}{4F/D} . \quad (2)$$

F/D is the focal ratio at the primary or secondary focus, depending on the configuration. If T_E is the edge taper in dB, then the maximum sidelobe level will be (for a Gaussian feed model)

$$P = 3.7 T_E \left(\frac{F}{D} \right)^2 10^{-T_E/10} . \quad (3)$$

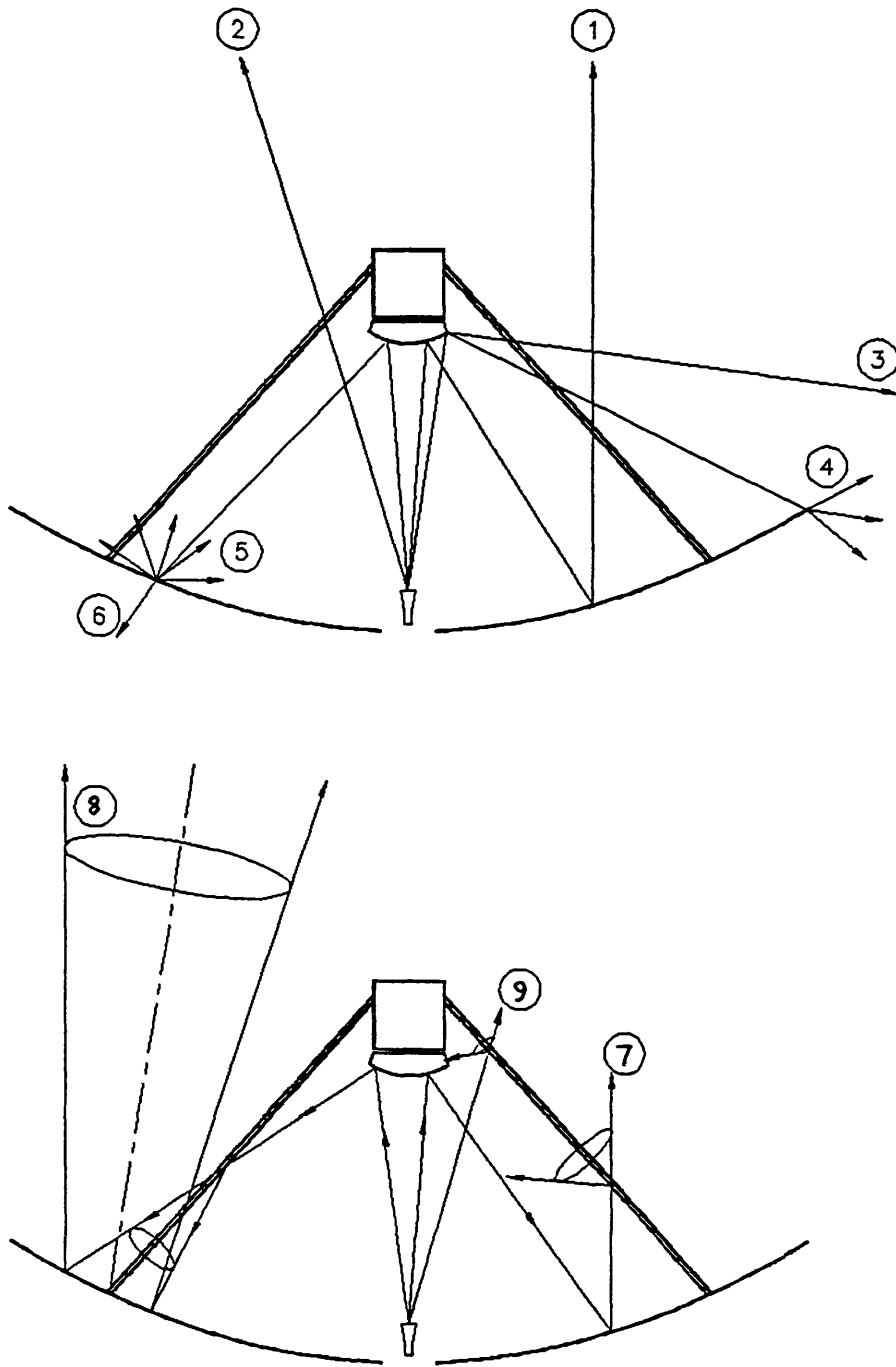


Figure 3 Some mechanisms resulting in sidelobes: (1)Near-in sidelobes, main beam, (2)spillover, (3)sec. diffraction, (4)prim. diffraction, (5)gap scattering, (6)gap trans,(7)plane wave scatt., (8)spher. wave scattering, (9)scattering of spillover power.

Taking as an example an edge taper of 10dB and an F/D of 7 gives a maximum sidelobe level of 22dBi at an angle of 4° to boresight. Long wavelengths would probably use a prime focus configuration with a lower focal ratio and a corresponding 20-30 dB reduction in levels. A focal ratio of 0.35 would result in a peak level of about -3dBi

Depending on the expected sources of sidelobe pickup, some compromise between level and angular distribution could be made by adjusting F/D, but since its range is probably determined by other considerations, T_E will be the main parameter for adjustment. Alternatively, absorber or metallic plates could be used to terminate or diffuse the spillover, but this would be at the expense of blockage in an on-axis system. Finally, more efficient feeds such as multimode corrugated horns could be used, perhaps, for particularly important frequencies.

Diffraction at the Secondary

In Cassegrain antennas the edge of the secondary produces a diffracted field which spills past the edge of the primary. An approximate treatment based on [2] gives the total spillover power as

$$P = \frac{-A_o \ln A_o}{\pi(1-A_o)} \sqrt{\frac{\lambda}{d}} \quad (4)$$

where A_o is the relative field amplitude at the edge of the secondary

$$A_o = 10^{-T_E/20} \quad (5)$$

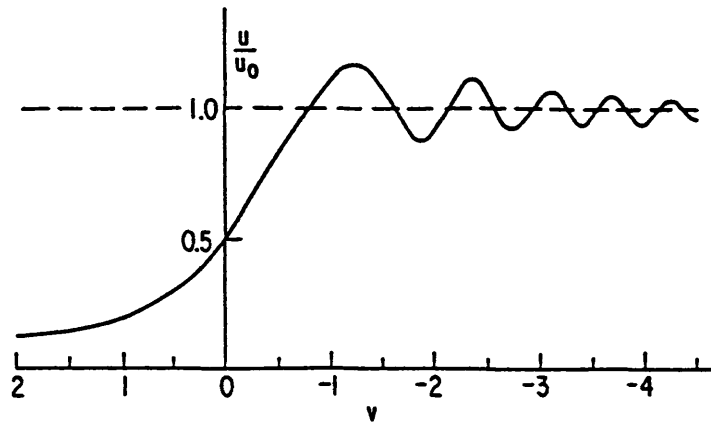
When $T_E = 10\text{dB}$, $d = 7\text{m}$, and $\lambda = 21\text{cm}$ then $P = -15\text{dB}$. The diffracted field falls off exponentially from the edge of the primary as a function of a dimensionless parameter v (Fig. 4) where

$$v = \theta \sqrt{\frac{d}{\lambda} \frac{f/D}{(1+(4f/D))^2}} \quad (6)$$

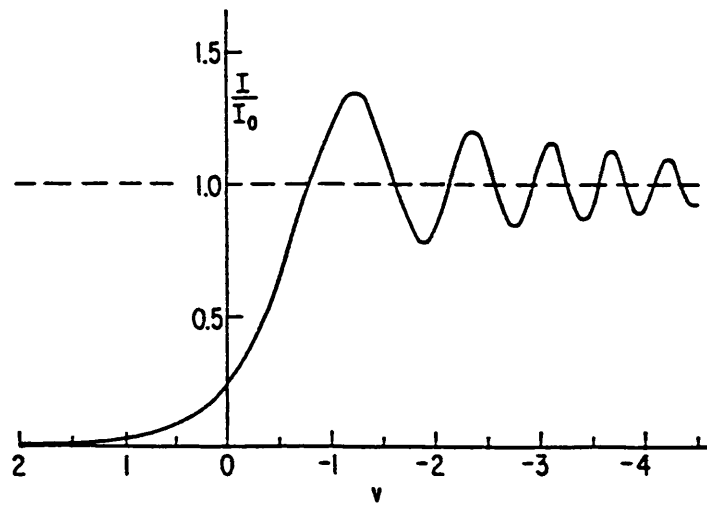
and θ is the radian angle away from the edge of the secondary. It is assumed that the edge of primary and secondary are lined up geometrically.

fe

As a measure for the extent of the pattern, assume the angle at which the intensity falls to 1% of its maximum value. This occurs when $v = 2.2$. For a primary



(a)



(b)

Plots of (a) amplitude and (b) intensity of the diffraction pattern of a straight edge in the far field.

Figure 4 Taken from [3]

focal ratio of 0.35

$$\theta = 3\sqrt{\frac{\lambda}{d}}. \quad (7)$$

This varies from about 40° for a 20 wavelength secondary to about 17° for a 100 wavelength secondary, for example.

The peak intensity will fall at the edge of the primary, where it will be 6dB less than the field expected from Geometrical Optics (GO). Assuming no diffraction by the rim of the primary, the intensity of the peak will be

$$P = 0.9T_E \left(\frac{f}{D}\right)^2 10^{-T_E/10} \quad (3)$$

relative to isotropic. When $f/D = 0.35$, $P = -10\text{dBi}$ for a 10dB edge taper. In practice, the second diffraction by the primary will reduce this peak value somewhat.

Diffraction at the Primary

Far-out sidelobes from the main aperture are due mainly to contributions from the outermost Fresnel zones since the inner zones cancel with adjacent zones. These sidelobes are therefore dependent primarily on the amplitude of the field at the rim. (For the purposes of this note, we neglect diffraction effects depending on the slope of the field.) To a first approximation, then, the sidelobe level may be estimated by using a circular aperture illuminated by a uniform field which is lower than the peak of the actual field by T_E dB. It is well known that a uniformly illuminated circular aperture has an Airy diffraction pattern [3]

$$P(\theta) = \left[\frac{2J_1(\pi D\theta/\lambda)}{\pi D\theta/\lambda} \right]^2 \quad (9)$$

The asymptotic envelope for this is

$$P(\theta) = 1.52 \times 10^5 \frac{\lambda}{D} 10^{-T_E/10} \theta^{-3} \quad (10)$$

with θ in degrees. When $D = 100\text{m}$, $\lambda = 21\text{cm}$, and $T_E = 10\text{dB}$, then $P(\theta) = 15 - 30\log \theta$ dBi.

The angle at which the intensity falls to the isotropic level is given by

$$\theta = 53 \left(\frac{\lambda}{D} 10^{-T_E/10} \right)^{1/3} \quad (11)$$

At $\lambda = 21\text{cm}$ and a 10dB edge taper the envelope falls to isotropic at about 3° .

The CCIR standard has a decay rate proportional to $\theta^{-2.5}$ rather than θ^{-3} , but this is intended to account for other sources of sidelobes, such as feed spillover.

Scattering by Gaps between Panels

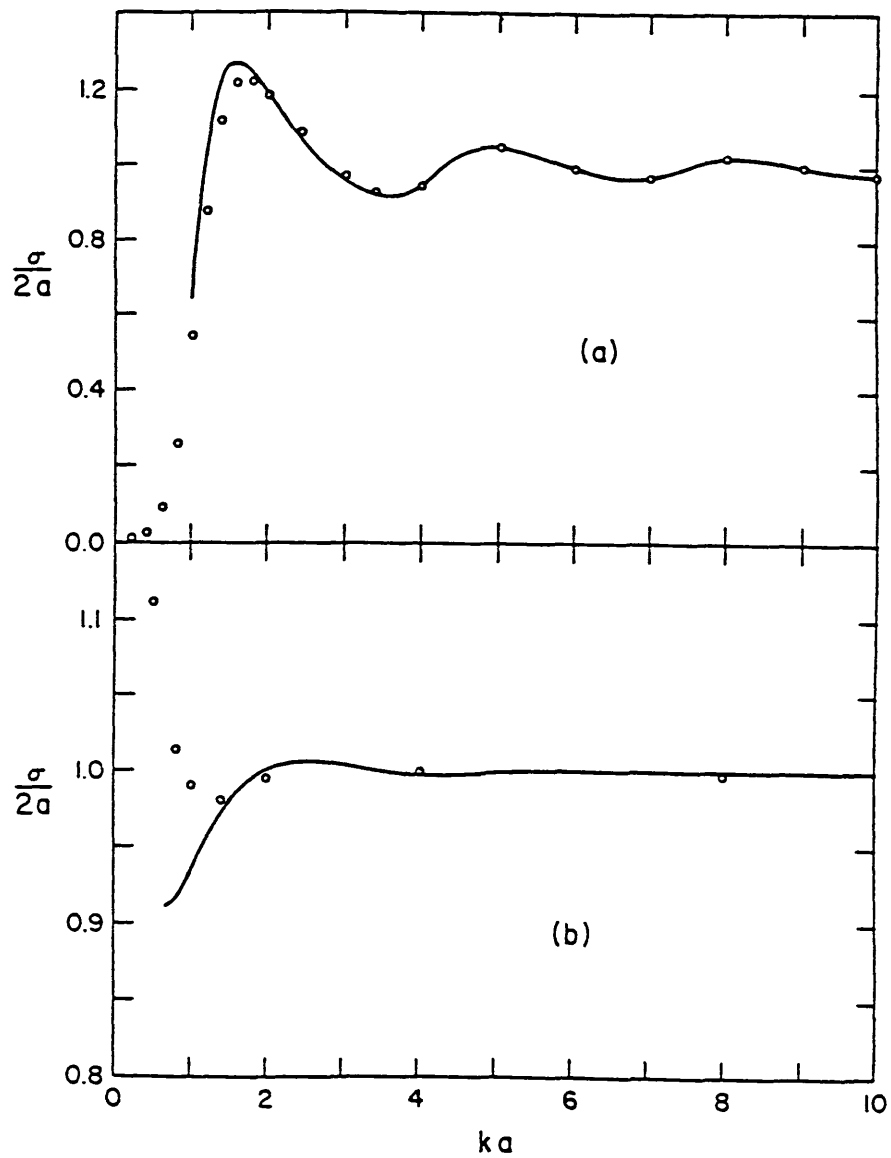
There is no simple analytical solution for the problem of a wave incident on a slit which has a width comparable to or smaller than a wavelength. Generally, it might be expected that the back scattered and transmitted fields will be distributed over a large angular range in a plane perpendicular to the gap axis. Furthermore, because the gap will affect parallel currents much less than transverse currents, the scattering will be very polarization dependent.

Exact and approximate calculation of the effective transmission cross-section of a slit have been done for slits as narrow as 0.06λ . Fig. 5 taken from Jull [4] shows that the effective size of the slit is within about 20% of the physical size down to about $g = 0.4\lambda$. Below this, the transmission for TE fields becomes negligible and the transmission for the TM fields increases rapidly. (The results do not indicate what happens at very small gap widths.)

As an educated guess, it is probably reasonable to assume the following:

- (a) The transmission of the gaps (averaged over the two polarizations) will be approximately equal to the fractional geometrical area of the grooves.
- (b) The back-scattered power will be approximately the same as the transmitted power.
- (c) The scattered and transmitted fields will be distributed over a wide range of angles and may be considered isotropic.

If p is a typical panel length, then the fractional area blockage will be $2g/p$. Approximately this fraction of the total power will be scattered over the forward hemisphere, and the same amount transmitted to the rearward hemisphere. The scattered power is then approximately



Transmission cross-section of a slit of width $2a$ for normal incidence of a plane wave.

a TE polarisation, eqn. 8.19

b TM polarisation, eqn. 8.25

o o Exact values (Skavlem, 1952)

(After Keller, 1957) ·

Figure 5 Transmission by a slit, from [4]

$$P = 4g/p . \quad (12)$$

Choice of the size of gap to leave between panels probably depends mainly on ease of installation of the panels, and on the magnitude of relative panel movements during use. Consider the thermal problem where the backing structure is steel with an expansion coefficient of 10^{-5}K^{-1} and an aluminum surface with a coefficient of $2.3 \times 10^{-5}\text{K}^{-1}$. Over a 50K temperature range there will be a relative change in length of about 0.07%. Changes in the gap size with gravitational deformation can be expected to be related to the deviation of the surface from the ideal and, therefore, on the shortest wavelength of the design, λ_{\min} . If the total distortion parallel to the surface is λ_{\min} then the fractional change in size will be λ_{\min}/D . As numerical examples, take a panel with a 2m linear dimension, and a maximum operating frequency of 46 GHz. The fractional change in dimension due to gravity will be approximately 0.007% and $g \approx 0.14\text{mm}$, while the thermal limit gives $g \approx 1.5\text{mm}$. In practice a value of around 3mm is probably acceptable, and the scattered power relative to isotropic would then be $P = -22\text{dB}$.

Most of the field leaking through the gaps will be terminated at ambient and add a small component to the antenna noise. It may be preferable to have explicit terminations in the way of absorber, so that there is no possibility of interference. Scattered power will fall uniformly on the sky mainly, and a component will also return to the feed producing a standing wave.

Scattering of Plane Wave by Struts

To estimate sidelobes due to the struts, we consider a strut of length L at an angle of β to the boresight direction and calculate the scattering of a uniform plane wave. Fig. 6 shows the strut-based coordinate system. The scattered field falls roughly into a conical pattern along a cone defined by $\theta_s = \beta$. When the strut is greater than a few wavelengths, ray tracing may be used to determine the ϕ_s distribution. In the orthogonal (θ_s) direction, the width of the pattern is diffraction-limited by the projection of the strut length on the aperture plane. If the strut length is L , then its projected length is

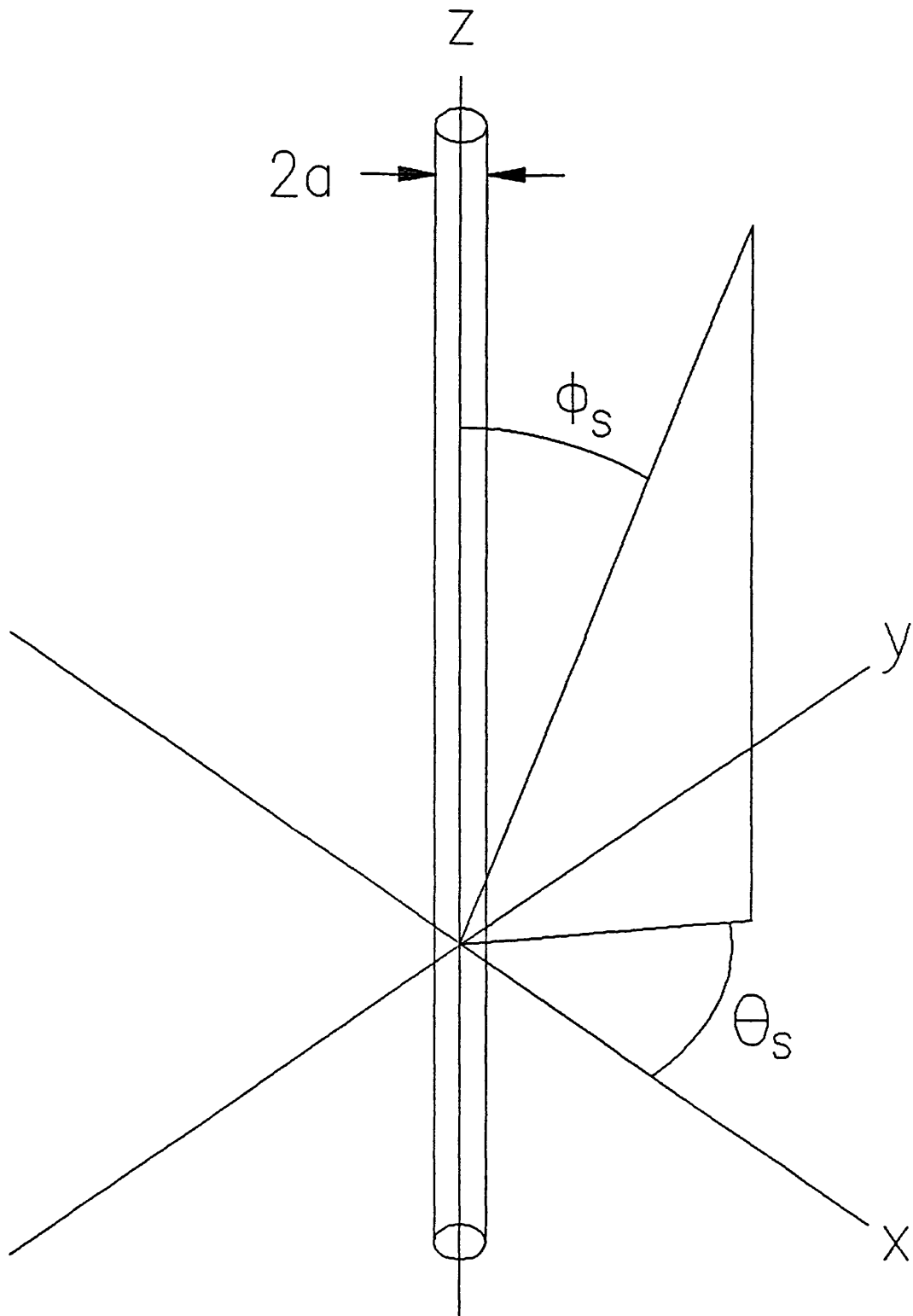


Figure 6 Coordinate system for strut as used in the text.

$$L_A = L \sin \beta , \quad (13)$$

and the scattered pattern for a circular cross-section of radius a is

$$P(\theta_s, \phi_s) = P_o \cos^2 \frac{\phi_s}{2} \frac{\sin^2(\pi L_A \theta_s / \lambda)}{(\pi L_A \theta_s / \lambda)^2} . \quad (14)$$

P_o is the peak amplitude relative to isotropic

$$P_o = \frac{8aL^2}{D^2} \frac{\sin \beta}{\lambda} . \quad (15)$$

Assuming some reasonable values as follows: $D = 100\text{m}$, $L = 41\text{m}$,
 $\beta = 40^\circ$, $a = 0.4\text{m}$, then

$$P_o = \frac{0.35}{\lambda} \quad (\lambda \text{ in m}) . \quad (16)$$

For $\lambda = 21\text{cm}$, this gives $P_o = 2.2\text{dBi}$. The total scattered power is

$$P = \frac{8aL_A}{\pi D^2} , \quad (17)$$

and for the above figures, this is about -24dB of the total power. This value must be increased in proportion to the number of struts in the design. Note that the peak power falls at an angle of 2β to the antenna boresight and is at the same azimuth direction as the leg.

The width of the pattern in the θ_s direction is

$$\Delta\theta = \frac{2\lambda}{L_A} . \quad (18)$$

Other Strut Cross-Sections

Rectangular struts will scatter the incident field at an angle of 2β to boresight and will have a distribution which is approximately

$$P(\theta_s, \phi_s) = P_o \frac{\sin^2(2\pi a \phi_s / \lambda)}{(2\pi a \phi_s / \lambda)^2} \frac{\sin^2(\pi L_A \theta_s / \lambda)}{(\pi L_A \theta_s / \lambda)^2} . \quad (19)$$

Since the spread of the beam is now much less, the peak level is much greater.

$$P_o = \left(\frac{8aL_A}{\lambda D} \right)^2 . \quad (20)$$

Taking the same values of parameters as in the previous section

$$P_o = \frac{0.71}{\lambda^2} \quad (\lambda \text{ in m}). \quad (21)$$

For a wavelength of $\lambda = 21\text{cm}$ this gives $P_o = 12.1\text{dBi}$

Since the direction of maximum scattering is usually in the direction of an opposing strut, the total scatter pattern will depend on a series of multiple scatterings. At the shorter wavelengths (less than a few centimeters), the scattering from a strut may be over a few degrees only so that an appreciable fraction could be re-scattered by the opposite strut. For example, an 80cm wide leg produces a scattered beam of about 2° at $\lambda 5\text{cm}$, while the opposing leg may subtend about 0.5° . Multiple scattering may also lead to standing wave problems.

Choosing an elliptical strut cross-section would distribute the energy around the cone more evenly than the circular cross-section. It would also permit a greater stiffness in the plane perpendicular to the aperture, which could be of significant advantage.

Long Wavelength Considerations

Although the above analysis uses GO ray tracing, there will be frequencies where GO is definitely not applicable. Because the strut length will be large compared to a wavelength, the pattern in the narrow (θ_s) direction will still have a width of about $2\lambda/L_A$ radians. When the width of the strut is comparable to a wavelength, the field will not see the details of the strut shape and the pattern around the cone will be approximately independent of the strut cross-sectional geometry.

The distribution around the cone will be approximately uniform. Rusch *et al.* have investigated strut scattering using Physical Optics (PO) [5] and their results agree broadly with the analysis done here. (There is some apparent discrepancy since I find the optical limit of their analysis gives a scattering which is uniform in ϕ rather than having the $\cos(\phi/2)$ dependence of (14). The disagreement is not significant as far as this note is concerned.)

An important result of the PO analysis is that the scattering is polarization dependent. When the E-field is in the plane of the strut, the scattering is greater than when the H-field is in the strut plane. At long wavelengths a strut in the H-plane becomes almost invisible. When there are struts in both planes the average effect will be roughly the same as if the blockage had been assumed to be equal to the geometrical area. However the sidelobe levels in the direction of the E-field struts will be larger than expected by $\sim 1-2$ dB.

Control of Strut Scattering

Obviously, the amount of energy scattered by the struts is minimized by making the struts as narrow as possible, but the improvement that can be made over any reasonable existing design is small ($\sim 2-3$ dB). This may be significant in terms of aperture efficiency, but less so as far as sidelobe level is concerned. As discussed in the previous section, the cross-sectional geometry can have a significant effect at the shorter wavelengths but not at longer ones. Straight struts were considered in the previous section, but the support structure could be composed of curved members or, more realistically, several straight members at different angles. If curved or segmented struts are used, the maximum deviation of the strut from a straight line needs to be greater than λ to broaden the scattering in the θ direction over the diffraction limit in (14). The JCMT is a good example of an antenna where the secondary support scattering is broken up by a structure with a number of narrow members at various angles [6].

Several other possibilities could be studied in detail. For example, using two support legs and guy wires (possibly dielectric) in the orthogonal plane could give reduced sidelobes for one linear polarization at low frequencies. (Was that observed on the 300'?) This option may not improve short wavelength operation, however. Dielectric struts are a possibility, but at short wavelengths there is no benefit since the strut will act as a cylindrical lens giving a wide-angle scattered pattern, or, if a rectangular section is used, the transmitted field could be retarded by π , *doubling* the

blockage over an opaque strut.) Finally, some type of truss comprising small members could be considered.

Scattering of Spherical Wave by Struts

A similar analysis may be applied to scattering of the spherical wave from the secondary, or prime focus feed. Typically, the amount of power scattered from the spherical wave is comparable to that scattered from the plane wave unless the legs are attached near the rim (probably impractical in a very large antenna). Each strut produces a cone which is then entirely reflected by the primary. The radiation on the sky will fall in a circular region passing through boresight (Fig. 5) and will be within an angle of

$$\theta_m = 2 \tan^{-1} (D/4f) - \beta \quad (22)$$

of the boresight direction. The width of the pattern varies from a diffraction limit of

$$\Delta\theta \approx \frac{4\lambda}{(D - 2r_b)} \quad (23)$$

near boresight, to

$$\Delta\theta \approx 2 \left(\tan^{-1} \left(\frac{D}{4f} \right) - \tan^{-1} \left(\frac{r_b}{2f} \right) \right) \quad (24)$$

At θ_m , r_b is the radius of the base of the strut on the primary reflector. This component of the strut scattering is, therefore, generally more diffuse than the scattering of the plane wave component, and the peak amplitudes will be correspondingly lower. Quantitatively, the peak will be on the order of

$$\frac{P_{(\text{spherical})}}{P_{(\text{plane})}} = \frac{\lambda}{L \sin\beta \left(\tan^{-1} \left(\frac{D}{4f} \right) - \tan^{-1} \left(\frac{r_b}{2f} \right) \right)} \quad (\lambda \ll L) \quad (25)$$

Taking as an example $r_b = 30\text{m}$, $L \sin\beta = 26\text{m}$, $f/D = 0.35$, and $D = 100\text{m}$ gives $P_{(\text{spherical})}/P_{(\text{plane})} = 0.15\lambda$, λ in meters. For $\lambda = 21\text{cm}$, $P_{(\text{spherical})}/P_{(\text{plane})} = -15\text{dB}$.

OFF-SET VS SYMMETRICAL

This section attempts to give a brief comparison of some estimates of the sidelobes of a symmetrical antenna and an off-set version. Clearly the methods used are approximate and no attempt has been made to do any kind of global optimization

Mechanism	Symmetrical		Off-Set	
	Total	Peak	Total	Peak
Feed Spillover	-18dB	12dBi	-20dB	8dBi
Secondary Diffraction	-20dB	-21dBi	-22dB	-25dBi
Primary Diffraction (at 10°)		-40dBi		-45dBi
Gaps Between Panels	-22dB	-22dBi	-22dB	-22dB
Plane Wave Scattering	-18dB	-10dBi	-	-
Spherical Wave Scattering	-18dB	-15dB	-	-
Total	-12dB		-16dB	

Table I Estimated integrated power and peak power in sidelobes due to various mechanisms. Assumes 21cm wavelength and edge tapers of 25dB and 30dB for the symmetrical and off-set antennas respectively.

in the available parameter space, but the results do give a feel for the magnitudes involved. Table I lists the calculated values for the integrated power in the sidelobes, and for the peak intensities at λ 21cm. For the example rather extreme values of the edge taper have been chosen: 25dB for the symmetrical case and 30 dB for the off-set. The larger taper has been allowed for the off-set than for the symmetrical antenna since narrowing the primary feed beam also increases the effect of the central

blockage of the secondary. In both cases the main beam is broadened which may or may not be acceptable in specific instances.

The strut scattering peak estimates are rather loose estimates made by assuming that a reduction of ~ 12 dB may be effected by using curved struts (possibly like the parabolic design of Siemens, built by MAN). This would seem to be quite feasible.

Looking at the Table it is clear that the total amount of power in the sidelobes is not very different between the two designs. The more noticeable difference is between the peak intensities, though even that amounts to only 7-8dB, excluding the feed spillover round the secondary. Spillover round the secondary of the off-set may be reflected by a collar either directly to the sky or *via* the primary, but this is not possible on the symmetrical antenna without incurring extra central blockage.

DISCUSSION AND CONCLUSIONS

Several mechanisms responsible for sidelobes have been identified and discussed in semi-quantitative detail. Generally it is relatively easy to estimate the total amount of power contained in the sidelobes but rather difficult to define the distribution precisely over the 4π sphere. It is apparent that the average amount of power in the sidelobes is in the range of -10 to -3 dB*i* and it is difficult to make any significant improvement in this. There is some flexibility in how the power is distributed, however, and this should be taken into account when a preliminary design is done.

Three main problems related to sidelobes may be identified (other than the question of the convolution of the near-in sidelobes with an extended source being observed). These are (a) increase of system noise due to sidelobes terminated at ambient, (b) pick-up of man-made interference, either from terrestrial sources or satellites, and (c) corruption of the observation by celestial sources other than that being measured, a typical example being galactic HI [7]. It is impossible to give a definitive answer to the question of the "best" sidelobe distribution because the importance of the various problems will depend on the wavelength of the observation, the type of measurement, and the nature of the source. Furthermore it is complicated by the fact that the distribution pattern is fixed to the telescope axes and therefore moves relative to terrestrial, solar, and sidereal sources (assuming an alt-az mount).

Interfering effects of celestial sources may be removed to some degree if the sidelobe and source distributions are known, and it is conceivable that this process would be easier to implement if the sidelobes were relatively strong and spatially limited (and therefore easily measured) rather than weak and diffuse. Of course a completely isotropic distribution would be the simplest to deconvolve, but it may be difficult to measure the pattern to ensure that it is isotropic.

Man-made interference is too variable to deconvolve and sidelobes should either avoid known sources, if possible, or be sufficiently diffuse to minimize pickup. Land based sources can be avoided if the sidelobes are towards the sky, but that may not be possible while observing low elevation sources and it would also increase the problems of satellite interference.

On the whole it appears that it is more desirable to have the sidelobes as diffuse as possible rather than concentrated in particular directions. Major causes of sidelobes are feed spillover (in a Cassegrain telescope) and strut scattering. Feed spillover in a Cassegrain may be reduced either by increasing the edge taper of the feed pattern or by using absorber or a reflecting shroud round the secondary. In an off-set configuration this may be done with no penalty in terms of extra blockage.

Strut scattering is entirely avoided in an off-set design, but steps may be taken in the case of the symmetrical antenna to reduce the peak intensity, and the improvement in going to an off-set design may not be much more than 10dB. In conclusion, there appears to be some advantage in going to an off-set geometry in terms of the far-out sidelobe response. However, improvements can be made even to the conventional design and the improvement in going to the off-set may be only on the order of 10db. Although the results given in this note are approximate they probably give a reasonable first order estimate of sidelobe levels and show how they can be optimized. A very limited part of the parameter space has been investigated and in particular only one frequency chosen but the equations presented should prove to be useful tools in an initial design. Numerical analysis will be needed to get better quantitative results and fine-tune the design, but even recent sophisticated methods may be limited as shown in [8] where supercomputer computations were used even for reflectors as small as 10λ .

REFERENCES

- [1] J. Ruze, "Antenna tolerance theory - a review", *Proc IEEE*, vol. 54 pp. 633-640, Apr. 1966.
- [2] P. S. Kildal, "The effects of subreflector diffraction efficiency on the aperture efficiency of a conventional Cassegrain antenna - an analytical approach", *IEEE Trans. Antennas Propagat.* vol. AP-31, no. 6, pp. 903-909, Nov. 1983.
- [3] M. Born and E. Wolf, *Principles of Optics*, Oxford: Pergamon Press, 1970.
- [4] E. V. Jull, *Aperture antennas and diffraction theory*, London: Peter Peregrinus, 1981.
- [5] W. V. T. Rusch, O. Sørensen, and J. W. M. Baars, "Radiation cones from feed-support struts of symmetrical paraboloidal antennas", *IEEE Trans. Antennas Propagat.*, vol. AP-30, no. 4, pp. 786-790, July 1982.
- [6] J. W. Lamb and A. D. Olver, "Blockage due to subreflector supports in large radiotelescope antennas", *Proc. IEE*, vol. 133, pt. H, no. 1, pp. 43-49, Feb 1986.
- [7] P. M. W. Kalberla, U. Mebold, and W. Reich, "Time variable 21 cm lines and the stray radiation problem", *Astron. Astrophys.*, vol. 82, pp. 275-286, 1980.
- [8] D. C. Jenn and W. V. T. Rusch, "An E-field integral equation solution for the radiation from reflector antennas with struts", *IEEE Trans Antennas Propagat.*, vol. 37, no. 6, pp. 683-9, June 1989.